Available online at www.sciencedirect.com

ScienceDirect

Journal of Photochemistry and Photobiology A: Chemistry 195 (2008) 183–190

Journal of Photochemistry and Photobiology A:Chemistry

www.elsevier.com/locate/jphotochem

Synthesis and solvent effects on the photophysicochemical properties of novel cadmium phenoxy phthalocyanines

Wadzanai Chidawanyika, Edith Antunes, Tebello Nyokong*

Department of Chemistry, Rhodes University, Grahamstown 6140, South Africa

Received 3 August 2007; received in revised form 26 September 2007; accepted 28 September 2007

Abstract

The syntheses of novel cadmium phenoxy complexes; tetrakis{1,(4)-*tert*-butylphenoxyphthalocyaninato}cadmium(II) (**5a**), tetrakis{1,(4)-phenoxyphthalocyaninato}cadmium(II) (**5b**), tetrakis{2,(3)-*tert*-butylphenoxyphthalocyaninato}cadmium(II) (**6a**) and tetrakis{2,(3)-phenoxyphthalocyaninato}cadmium(II) (**6b**) are presented herein. The spectroscopic and photophysicochemical properties have also been carried out and discussed together with the influence of various organic solvents on these properties. Spectroscopic properties, i.e. ground state electronic absorption and fluorescence spectra have been found to vary as a function of substituent position on the phthalocyanine macrocycle, i.e. α-substitution versus β-substitution. The photophysical parameters are reported as well as the photodegradation and singlet oxygen quantum yields, where the complexes were found to exhibit good photostability with the production of appreciable amounts of singlet oxygen.

Keywords: Cadmium phthalocyanine; Fluorescence quantum yields; Solvent effects; Photodegradation; Singlet oxygen quantum yields; Triplet lifetimes

1. Introduction

Since their discovery in the early 1900s, metallophthalocyanines (MPcs) have attracted much interest [1–7] due to their high chemical and thermal stability, high degree of aromaticity, synthetic flexibility and ability to adapt to a wide range of applications. MPcs exhibit intense absorption towards the red end region of the visible spectrum where the wavelength varies depending on the central metal and the type, number and position of substituents attached to the phthalocyanine macrocycle [8]. Extensive studies on tetra-substituted complexes have shown that non-peripheral (α) substitution results in a more red shifted Q-band compared to peripheral (β) substitution, as a result of the much larger linear combination of atomic orbital coefficients at the carbon atoms at α-positions relative to those at the β-positions [8–10].

We have recently reported on the synthesis and photophysical characterization of tetrakis{2,(3)-pyridyloxyphthalocyaninato} zinc, cadmium and mercury complexes [11]. This study showed the CdPc and HgPc derivatives to have very low triplet lifetimes in dimethylsulphoxide and the CdPc and ZnPc complexes were found to be highly aggregated in some solvents. With the aim of improving the photophysical behaviour of CdPc derivatives, we report herein on the synthesis, photophysical and photochemical behaviour of novel tetrakis{1,(4)-phenoxyphthalocyaninato}, tetrakis{1,(4)-*tert*-butylphenoxyphthalocyaninato}, tetrakis{2,(3)-phenoxyphthalocyaninato} and tetrakis{2,(3)-*tert*-butylphenoxyphthalocyaninato} complexes of cadmium. Although toxic, Cd and Hg type complexes have been studied so as to provide a more complete study of the d^{10} metal group, since the corresponding Zn phthalocyanine derivatives have been studied extensively. Also Cd and Hg phthalocyanine derivatives may be useful as photocatalysts in some chemical transformations. The addition of substituents to the peripheral (β) and non-peripheral (α) positions of the MPc ring is expected to give enhanced solubility in numerous organic solvents [6,12] and affect the electronic spectra and triplet state properties.

---

* Corresponding author. Tel.: +27 46 6038260; fax: +27 46 6225109.
E-mail address: t.nyokong@ru.ac.za (T. Nyokong).

1010-6030/$ – see front matter © 2007 Elsevier B.V. All rights reserved.
doi:10.1016/j.jphotochem.2007.09.020

Table 1
Variation of Q-band λ_{max} of **5b** in solvents with varying properties

Solvent	Dipole moment, μ	Refractive index, η_D	Viscosity	Basicity[a]	Donor no.[b] (kcal mol^{-1})	Q-band, λ_{max} (nm)
Toluene	0.38	1.097	0.59	0.128	–	694
THF	1.69	1.406	0.55	0.591	20.0	693
Chloroform	1.90	1.438	0.57	0.071	0.00	700
DMF	3.79	1.430	0.92	0.613	26.6	694
DMSO	3.96	1.479	2.00	0.647	29.8	698

[a] Values from refs. [34,43].

[b] Values from refs. [44,45].

Depending on their properties (Table 1), solvents may also lead to changes in photochemical and photophysical behaviour [13,14] of MPcs, hence solvent effects on these properties are explored in this work.

2. Experimental

2.1. Materials

The solvents, chloroform ($CHCl_3$), *N*,*N*-dimethylformamide (DMF), dimethylsulphoxide (DMSO), methanol (MeOH), 1-octanol, tetrahydrofuran (THF) and toluene were obtained commercially, dried and/or distilled prior to use. Cadmium acetate, deuterated chloroform ($CDCl_3$), deuterated dimethylsulphoxide (DMSO-d_6), 1,8-diazabicylco[5.4.0]undec-7-ene (DBU), 1,3-diphenylisobenzofuran (DPBF), 4-*tert*-butylphenol, 4-nitrophthalonitrile, 4-phenol, potassium carbonate (K_2CO_3), silica gel 60, silica gel 60 P F_{254} and trifluoroacetic acid (TFA) were purchased from Aldrich and used as received. Column chromatography was performed on silica gel 60 (0.04–0.063 mm). Preparative thin layer chromatography was performed on silica gel 60 P F_{254}.

2.2. Equipment

FT-IR spectra (KBr pellets) were recorded on a Perkin-Elmer spectrum 2000 FT-IR spectrometer. Ground state electronic absorption spectra were recorded on a Varian Cary 500 UV–vis-NIR spectrophotometer; and ^{1}H NMR spectra on Bruker AMX 400 and Bruker AVANCE II +600 MHz spectrometers. Fluorescence emission and excitation spectra were recorded on a Varian Cary Eclipse spectrofluorimeter. Elemental analyses were carried out by the University of Cape Town. Triplet absorption and decay kinetics were recorded on a laser flash photolysis system, the excitation pulses were produced by a Nd: YAG laser (Quanta-Ray, 1.5 J/90 ns) pumping a dye laser (Lambda Physic FL 3002, Pyridin 1 in methanol). The analyzing beam source was from a Thermo Oriel xenon arc lamp, and a photomultiplier tube was used as the detector. Signals were recorded with a two-channel digital real-time oscilloscope (Tektronix TDS 360); the kinetic curves were averaged over 256 laser pulses. Triplet lifetimes were determined by exponential fitting of the kinetic curves using OriginPro 7.5 software.

Photo-irradiations were done using a General electric Quartz line lamp (300 W). A 600 nm glass cut off filter (Schott) and a water filter were used to filter off ultraviolet and infrared radiations, respectively. An interference filter (Intor, 670 nm with a band width of 40 nm) was additionally placed in the light path before the sample. Light intensities were measured with a POWER MAX 5100 (Molelectron detector incorporated) power meter.

2.3. Syntheses and characterization

3,(4)-*tert*-Butylphenoxyphthalonitrile (**3a**), 3-phenoxyphthalonitrile (**3b**), 4,(4)-*tert*-butylphenoxyphthalonitrile (**4a**) and 4-phenoxyphthalonitrile (**4b**) were synthesized and characterized as reported before [15,16].

2.3.1. Tetrakis{1,(4)-tert-butylphenoxyphthalocyaninato}cadmium(II)—5a

A mixture of **3a** (1.38 g, 5.00 mmol), cadmium acetate (0.50 g, 1.25 mmol) and DBU (5 mmol) was heated to 140 °C in 1-octanol (10 ml) under a dry, inert atmosphere (N_2) for 6 h. On cooling, the dark green solution was added to MeOH (∼50 ml), filtered and chromatographed using silica-gel 60, and THF as the eluting solvent. A dark green solid was obtained once the solvent was removed by evaporation. Yield: 0.35 g (24%). UV/vis (DMSO): λ_{max} nm (log ε): 329 (4.96), 629 (4.78), 698 (5.48). IR [(KBr) υ_{max}/cm^{-1}]: 2954 ($\upsilon_{C–H}$), 1266 ($\upsilon_{C–O–C}$).

^{1}H NMR (600 MHz, $CDCl_3$): δ, ppm; 7.79 (d, J = 8.09 Hz, 4H, Pc–H), 7.74 (br s, 3H, Pc–H), 7.43 (t, J = 8.46 Hz, 8H, Pc–H/Ar–H), 7.30 (m, 5H, Ar–H), 7.24–7.28 (m, 4H, Ar–H), 7.08 (d, J = 8.56 Hz, 8H, Ar–H), 1.35 (s, 36H, t-CH_3). Anal. Calcd. for $CdC_{72}N_8O_4H_{64}$: C (71.02), H (5.30); found: C (72.72), H (6.11).

2.3.2. Tetrakis{1,(4)-phenoxyphthalocyaninato}cadmium(II)—5b

A similar synthetic and purification procedure as for **5a**, was followed for **5b** using: **3b** (1.10 g, 5.00 mmol), cadmium acetate (∼0.50 g, 1.25 mmol excess) and DBU (5 mmol) in 1-octanol (10 ml). Yield: 0.61 g (49%). UV/vis (DMSO): λ_{max} nm (log ε): 351 (4.73), 631 (4.56), 698 (5.26). IR [(KBr) υ_{max}/cm^{-1}]: 2912 ($\upsilon_{C–H}$), 1244 ($\upsilon_{C–O–C}$); ^{1}H NMR (600 MHz, $CDCl_3$): δ, ppm; 7.79 (d, J = 8.09 Hz, 4H, Pc–H), 7.74 (br s, 3H, Pc–H), 7.43 (t, J = 8.46 Hz, 8H, Pc–H/Ar–H), 7.30 (m, 5H, Ar–H), 7.24–7.28 (m, 4H, Ar–H), 7.08 (d, J = 8.56 Hz, 8H, Ar–H). Anal. Calcd. for $CdC_{56}N_8O_4H_{32}$: C (67.71), H (3.25); found: C (68.29), H (3.35).

2.3.3. Tetrakis{2,(3)-tert-butylphenoxyphthalocyaninato}cadmium(II)—6a

Following a similar synthetic and purification procedure as in **5a**, **6a** was prepared using: **4a** (1.38 g, 5.00 mmol), cadmium acetate (0.50 g, 1.25 mmol excess) and DBU (5 mmol) in 1-octanol (10 ml). Yield: 0.25 g (17%). UV/vis (DMSO): λ_{max} nm (log ε): 355 (5.08), 613 (4.80), 684 (5.47). IR [(KBr) υ_{max}/cm^{-1}]: 2955 ($\upsilon_{C–H}$), 1235 ($\upsilon_{C–O–C}$); ^{1}H NMR (600 MHz, CDCl$_3$): δ, ppm 7.82–7.73 (br s, 2H, Pc–H), 7.69 (dd, $J = 5.69$, 3.31 Hz, 2H, Pc–H), 7.57 (m, 3H, Pc–H), 7.51 (m, 5H, Pc–H), 7.42–7.40 (m, 7H, Ar–H), 7.06–7.03 (m, 9H, Ar–H), 1.33 (s, 36H, t-CH$_3$). Anal. Calcd. For $CdC_{72}N_8O_4H_{64}$: C (71.02), H (5.30); found: C (72.23), H (6.38).

2.3.4. Tetrakis{2,(3)-phenoxyphthalocyaninato}cadmium(II)—**6b**

Following a similar synthetic and purification procedure as in **5a**, **6b** was prepared using: **4b** (1.15 g, 5.22 mmol), cadmium acetate (0.50 g, 1.25 mmol excess) and DBU (5 mmol) in 1-octanol (10 ml). Yield: 0.23 g (18%). UV/vis (DMSO): λ_{max} nm (log ε): 350 (4.83), 613 (4.61), 681 (5.22). IR [(KBr) υ_{max}/cm^{-1}]: 3167–3061 ($\upsilon_{C–H}$), 1232 ($\upsilon_{C–O–C}$); ^{1}H NMR (600 MHz, CDCl$_3$): δ, ppm 7.70–7.09 (m). Calcd. for $CdC_{56}N_8O_4H_{32}$: C (67.71), H (3.25); found: C (68.58), H (3.85).

2.4. Photochemical and photophysical studies

2.4.1. Singlet oxygen quantum yields

Singlet oxygen quantum yield (Φ_Δ) values were determined in air using the relative method with DPBF acting as a singlet oxygen chemical quencher in DMSO, using Eq. (1):

$$\Phi\Delta = \Phi_\Delta^{Std} \frac{R\, I_{abs}^{Std}}{R^{Std}\, I_{abs}} \tag{1}$$

where Φ_Δ^{Std} is the singlet oxygen quantum yield for the ZnPc standard ($\Phi_\Delta^{Std} = 0.56$ in DMF [17], 0.67 in DMSO [18], 0.53 in THF [19] and 0.58 in toluene [20]); R and R^{Std} are the DPBF photobleaching rates in the presence of the respective MPc and standard, respectively; I_{abs} and I_{abs}^{Std} are the rates of light absorption by the MPc and standard, respectively. The light intensity used for Φ_Δ determinations was found to be 2.97×10^{16} photons s^{-1} cm^{-2}; and the error in the determination of Φ_Δ was ~10% (from several Φ_Δ values). Chain reactions induced by DPBF in the presence of singlet oxygen often occur [18], therefore the concentration of DPBF was lowered to $\sim 3 \times 10^{-5}$ mol dm^{-3} for all solutions. DPBF degradation was monitored at 417 nm.

The fraction of the excited triplet state quenched by ground state molecular oxygen, S_Δ was calculated using Eq. (2):

$$S_\Delta = \frac{\Phi_\Delta}{\Phi_T} \tag{2}$$

2.4.2. Photodegradation quantum yields

For the determination of photodegradation quantum yields (Φ_{Pd}), Eq. (3) was employed:

$$\Phi_{Pd} = \frac{(C_0 - C_t)VN_A}{I_{abs}St} \tag{3}$$

where C_0 and C_t (mol dm^{-3}) are the respective CdPc derivative's concentrations before and after irradiation, respectively; V is the reaction volume; S the irradiated cell area (2.0 cm^2); N_A, the Avogadro's number; t, the irradiation time (in seconds) and I_{abs}, the overlap integral of the radiation source intensity and the absorption of the MPc.

2.4.3. Fluorescence quantum yields

Fluorescence quantum yields (Φ_F) were determined by the comparative method [21,22] (Eq. (4)),

$$\Phi_F = \Phi_{F(Std)} \frac{F\, A_{Std}\, \eta^2}{F_{Std}\, A\, \eta_{Std}^2} \tag{4}$$

where F and F_{Std} are the areas under the fluorescence curves of the MPc and the reference, respectively. A and A_{Std} are the absorbances of the sample and reference at the excitation wavelength, respectively, and η and η_{Std} are the refractive indices of solvents used for the sample and reference, respectively. Chlorophyll a in ether ($\Phi_F = 0.32$ [23]) was employed as a reference. Both the sample and reference were excited at the same wavelength (610 nm). The absorbance of the solutions at the excitation wavelength ranged between 0.04 and 0.05.

2.4.4. Triplet quantum yields and lifetimes

The de-aerated solutions of the respective MPc complexes were introduced into a 1 cm pathlength spectrophotometric cell and irradiated at the Q-band with the laser system described above. Triplet quantum yields (Φ_T) of the MPc complexes were determined by the triplet absorption method. A comparative method [24] using ZnPc as standard was employed for the calculations, Eq. (5).

$$\Phi_T = \Phi_T^{Std} \frac{\Delta A_T\, \varepsilon_T^{Std}}{\Delta A_T^{Std}\, \varepsilon_T} \tag{5}$$

where ΔA_T and ΔA_T^{Std} are the changes in the triplet state absorbances of the MPc derivative and the standard, respectively; ε_T and ε_T^{Std}, the triplet state molar exctinction coefficients for the MPc derivative and the standard, respectively; Φ_T^{Std}, the triplet quantum yield for the standard ($\Phi_T^{Std} = 0.65$ for ZnPc in DMSO [25], 0.58 for ZnPc in DMF [26] and 0.65 for ZnPc in toluene [27]).

Triplet lifetimes (τ_T) were determined by exponential fitting of the kinetic curves using OriginPro 7.5 software.

Quantum yields of internal conversion (Φ_{IC}) were obtained from Eq. (6), which assumes that only the three intrinsic processes (fluorescence, intersystem crossing and internal conversion), jointly deactivate the excited singlet state of an MPc molecule.

$$\Phi_{IC} = 1 - (\Phi_F + \Phi_T) \tag{6}$$

3. Results and discussion

3.1. Syntheses and characterisation

The general procedure for synthesis of substituted phthalonitrile derivatives has been well documented [28,29] and the preparation of the substituted phenoxy derivatives was carried

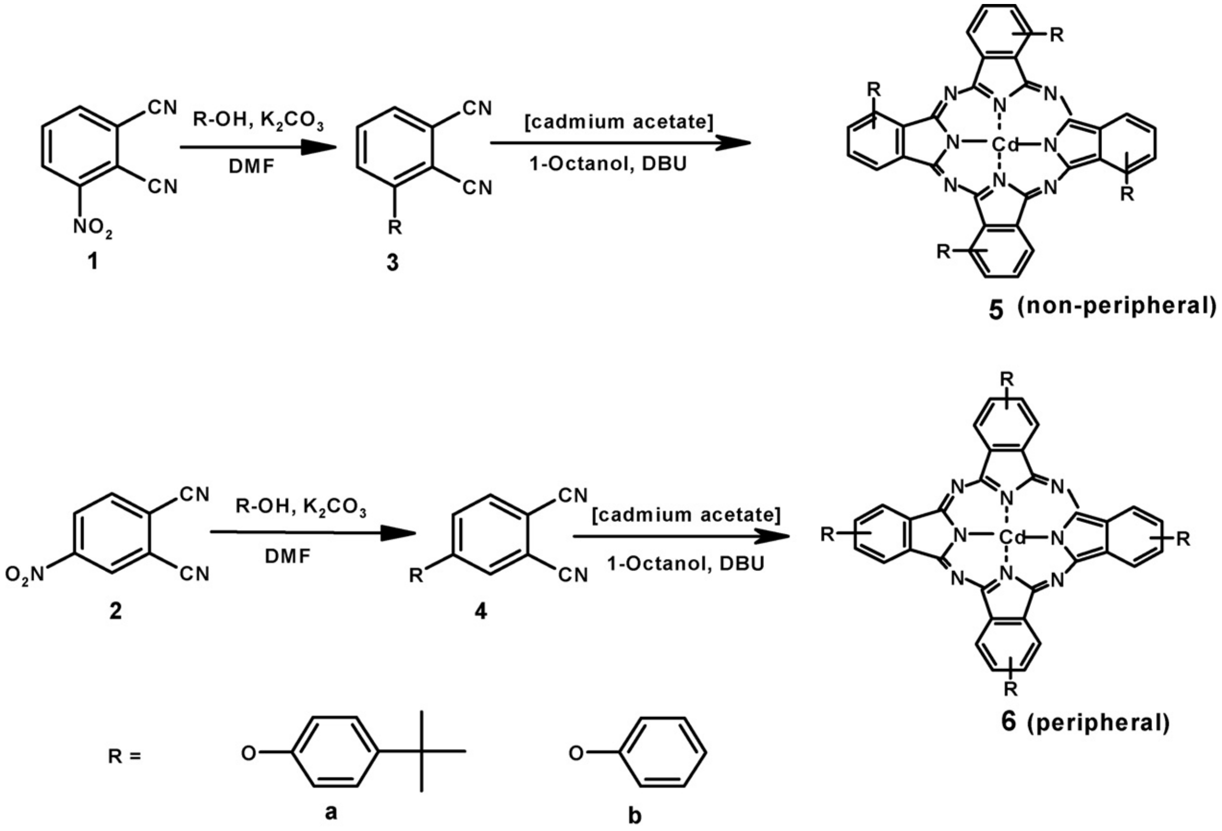

Scheme 1. Syntheses of cadmium complexes **5a**, **5b**, **6a** and **6b**.

out as reported before [15,16] (Scheme 1). Cyclotetramerisation of the substituted phthalonitrile derivatives (**3a**, **3b**, **4a**, **4b**), occurs under reflux conditions using a high boiling point solvent, i.e. 1-octanol and cadmium acetate. Chlorinated metal salts tend to form halogenated phthalocyanine contaminants and are therefore generally avoided [6]. All complexes formed are tetra-substituted; however, the use of different MPc precursors (3-nitrophthalonitrile or 4-nitrophthalonitrile) results in substitution patterns at different points of the MPc macrocycle, i.e. α- or β-substituted MPcs, each with their own unique solution and solid-state properties [6]. Purification procedures to obtain pure products were simple, but tend to give low yields typically varying between 15 and 40%.

It is well known that the solubility of phthalocyanines is poor in most common organic solvents [6], however, tetra-substitution is known to produce positional isomers which lead to enhanced solubility. Complexes **5a**, **5b**, **6a** and **6b** all exhibit excellent solubility (up to 1×10^{-4} mol dm^{-3}) in toluene, THF, $CHCl_3$, DMF and DMSO.

Characterisation of the newly developed complexes was carried out using IR, UV–vis and ^{1}H NMR spectroscopies and elemental analyses and was in agreement with the predicted structures. IR spectra depicts the disappearance of the characteristic nitrile stretch (C≡N) of phthalonitrile derivatives (**3a**, **3b**, **4a** and **4b**) at ~2230 cm^{-1} on formation of the metal-substituted Pc macrocycles. Vibrations due to the ether groups (C–O–C) occur between 1230 and 1270 cm^{-1} for the CdPc derivatives. The ^{1}H NMR spectra of the complexes show complex patterns in some cases due to the presence of mixed isomers. This is especially true for complex **6b** which showed only overlapping peaks, hence could not be integrated correctly, but good elemental analyses results were obtained. The ^{1}H NMR spectra of **5a** and **5b** are identical. The differences in the chemical shifts of the ^{1}H NMR spectra of complexes **5** and **6** is a function of the different substitution patterns, i.e. α-substituted (non-peripheral) phenoxy complexes versus the β-substituted (peripheral) phenoxy complexes as well as the type of the substituents introduced at these positions.

3.2. Ground state electronic absorption and fluorescence spectra

The ground state electronic absorption spectra for **5a** and **6a** in DMSO are shown in Fig. 1a and that of the corresponding to **5b** and **6b** in Fig. 1b. These display a sharp, intense single Q-band maxima of the complexes depicting their monomeric behaviour (for up to 1×10^{-5} mol dm^{-3}) in all solvents used for this study. The shoulders to the higher energy side of the main Q-band are vibronic. This is contrary to the reported [11] behaviour of Cd tetra{2,(3)-pyridyloxyphthalocyanine which was highly aggregated in chloroform even at very low concentrations. Thus the phenoxy derivatives seem to improve on the aggregation behaviour of CdPc derivatives. Due to the high atomic orbital coefficients of carbon atoms at the α-positions [8–10], the α-substituted derivatives (**5**) occur with spectra red-shifted relative to that of the β-derivatives (Fig. 1; Table 2).

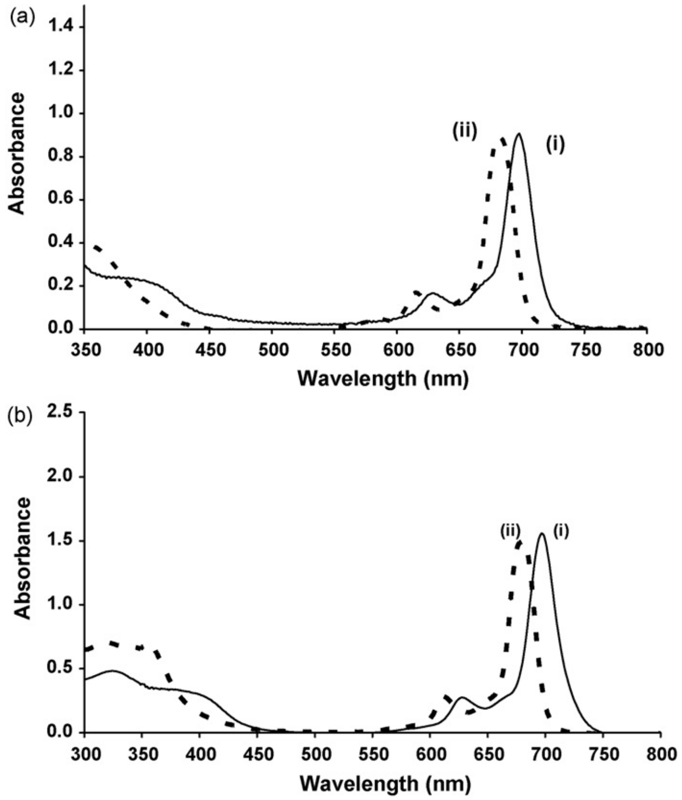

Fig. 1. Ground state electronic absorption spectra of (a) **5a** (i) and **6a** (ii) (concentration = $\sim 1.5 \times 10^{-5}$ mol dm^{-3}) and (b) **5b** (i) and **6b** (ii) (concentration = $\sim 8.0 \times 10^{-6}$ mol dm^{-3} in DMSO).

Substitution at the α-positions gives a larger destabilisation of the highest occupied molecular orbital (HOMO), resulting in a smaller HOMO-LUMO band separation, the extent of which is further enhanced on the introduction of electron donating groups such as the phenoxy and *tert*-butylphenoxy groups employed in this work [8]. For example, the Q-band of unsubstituted CdPc in DMSO occurs at 679 nm, while complex **5b** shows the Q-band at 698 nm in the same solvent. Complexes **5a** and **5b** experience a 14–19 nm bathochromic shift relative to **6a** and **6b** in all solvents. As observed in Table 2, a change in the solvent is also accompanied by a change in the position of the Q-band. It has been suggested previously that the solvent's refractive index affects its Q-band maxima [13,20]. However, it has also been shown that the nature, position and number of the substituents attached to the Pc macrocycle, as well as the metal centre may also exert some influence on the position of the Q-band [8]. It has been suggested that in the presence of coordinating solvents, e.g. DMSO, the interaction that occurs between the solvent and the Pc molecule tends to stabilise the lowest unoccupied molecular orbital (LUMO) [13] resulting in a smaller HOMO-LUMO separation which accounts for the long Q-band maxima in this solvent, Table 2, compared to the rest of the solvents (with the exception of complexes **5** in $CHCl_3$).

All complexes (**5a**, **5b**, **6a** and **6b**) showed a small band between 740 and 750 nm, Fig. 2 (curve i). In literature, this has been referred to as the 'X' band, a feature which has been attributed to the flexible σ attachment of phenoxy (C–O–C) groups at the Pc-periphery [30–32]. This flexibility allows the groups to 'twist' about the bond and induce a slight loss in symmetry, hence splitting the Q-band [33]. However, this band was not observed in DMSO and DMF and it was observed only for complexes **5** (non-peripherally substituted) in THF, chloroform and toluene. Thus this band is solvent dependant

Table 2
Photophysicochemical parameters of CdPc derivatives

Solvent	MPc	λ_{max} (nm)	log ε	Φ_F	Φ_T[a]	Φ_{IC}[a]	Φ_Δ	S_Δ[a]	$\Phi_{Pd}/10^5$
Toluene	**5a**	694	5.39	0.27	0.49	0.24	0.40	0.82	1.80
	5b	694	5.21	0.054	0.73	0.22	0.58	0.79	2.53
	6a	681	5.38	0.14	0.76	0.10	0.33	0.43	0.92
	6b	681	5.15	0.13	0.87	0.00	0.32	0.37	0.98
THF	**5a**	693	5.36	0.50			0.44		1.67
	5b	693	5.14	0.47			0.43		4.01
	6a	678	5.34	0.27			0.27		0.069
	6b	677	5.13	0.29			0.31		2.72
$CHCl_3$	**5a**	700	5.44	0.49			0.49		3.30
	5b	700	5.23	0.39			0.31		2.20
	6a	681	5.43	0.27			0.19		3.84
	6b	681	5.18	0.27			0.19		4.40
DMF	**5a**	694	5.46	0.53	0.56	0.09	0.56	1.00	2.13
	5b	694	5.25	0.31	0.49	0.20	0.42	0.86	3.89
	6a	678	5.46	0.32	0.41	0.27	0.26	0.63	2.47
	6b	677	5.22	0.29	0.40	0.31	0.39	0.97	3.55
DMSO	**5a**	698	5.48	0.055	0.61	0.34	0.59	0.97	0.19
	5b	698	5.26	0.063	0.66	0.28	0.80	1.21	2.86
	6a	684	5.47	0.21	0.54	0.25	0.35	0.65	0.41
	6b	681	5.23	0.20	0.61	0.19	0.41	0.67	0.42

[a] Values in some solvents could not be determined due to lack of reference standards.

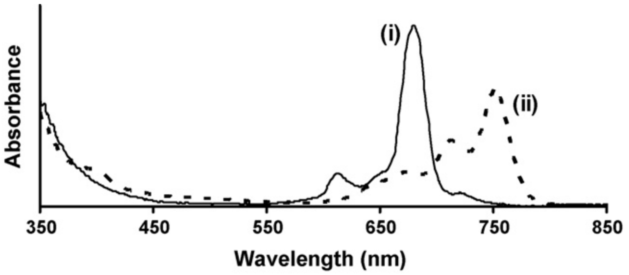

Fig. 2. Protonation of **6b** (concentration = ~4.0×10^{-6} mol dm^{-3}) in $CHCl_3$ using trifluoroacetic acid (TFA). Spectra in the absence (i) and presence (ii) of 2.0×10^{-3} mol dm^{-3} TFA.

hence may not be due to the phenoxy group twisting discussed above.

Toluene and THF also have small amounts of acid (hence the 'X' band is observed in these solvents). In DMSO and DMF the band is not observed since these solvents do not contain acid. Fig. 2 shows the expected spectral changes due to protonation of **6b** using trifluoroacetic acid (TFA), a protonating agent. The figure shows the enhancement of the band at 750 nm on protonation, thus confirming that this band may be due to protonation. The band near 750 nm was observed for complexes **6** only in chloroform while it was observed for complexes **5**, in THF, toluene and chloroform. This shows that substitution at the non-peripheral substitution is more prone to protonation than at the peripheral positions.

Fluorescence emission and excitation spectra typical of MPc derivatives were observed for the β-substituted MPc complexes and confirmed the presence of monomeric fluorescent species. For complexes **6**, the fluorescence spectra were mirror images of the absorption spectra (which are in turn are similar to the excitation spectra) in all solvents (Fig. 3). A large splitting of the Q-band was observed in the emission spectra for complexes **5** in chloroform, toluene and THF, Fig. 4, showing that upon excitation, the loss of symmetry becomes more enhanced as shown by the presence of the much higher intensity of the "X" band (Fig. 4). Again this shows that non-peripheral substitution is affected by protonation to a larger extent, which also affects emission spectra.

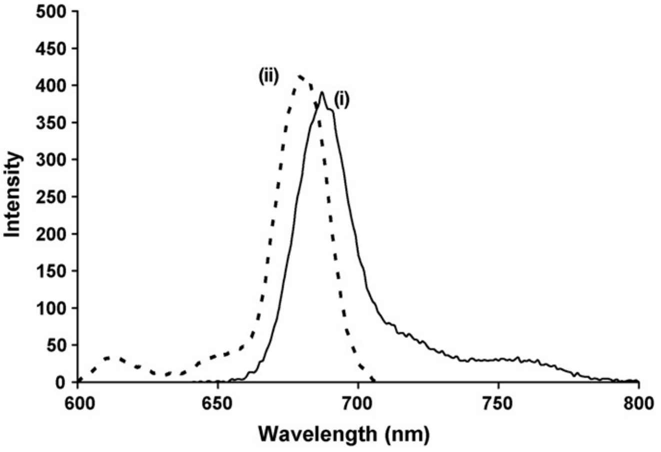

Fig. 3. Fluorescence emission (i) and excitation spectra (ii) of **6b** in toluene. Concentration: ~7.5×10^{-7} mol dm^{-3}; excitation wavelength (λ_{exc}) for emission = 610 nm; emission wavelength for excitation spectrum was 698 nm.

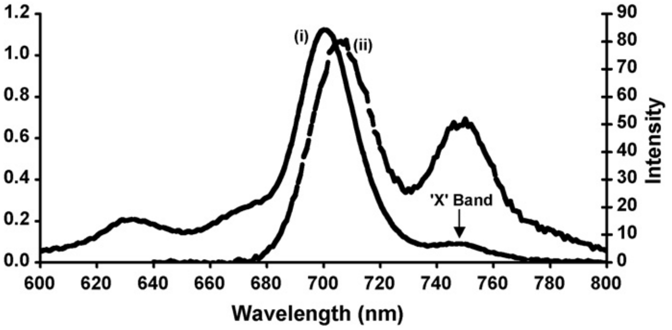

Fig. 4. Absorption (i) and fluorescence emission spectra (ii) of **5a** in $CHCl_3$. Concentration: ~7.5×10^{-7} mol dm^{-3}; excitation wavelength (λ_{exc}) for emission = 610 nm.

3.3. Photochemical studies

3.3.1. Singlet oxygen quantum yields

Singlet oxygen ($^1\Delta_g$) is believed to be the 'chief' cytotoxic species generated from the interaction between the triplet state photosensitiser (MPc) and ground state molecular oxygen ($^3\Sigma_g$). The reaction involves an energy transfer mechanism. The quantum yield of singlet oxygen (Φ_Δ) thus varies as a function of the triplet state properties of the respective MPc molecules, i.e. triplet state quantum yield, triplet state lifetime, triplet energy (E_T), energy transfer efficiency (quantified by S_Δ) and substituent quenching abilities. Triplet state yields (hence singlet oxygen quantum yields) are affected by the nature of the metals. Heavy metals increase intersystem crossing, hence the triplet state yield. Table 2 shows that the α-substituted phenoxy and *tert*-butylphenoxy CdPc derivatives (**5a** and **5b**) show higher Φ_Δ values than their corresponding β-substituted derivatives. Solvent effects (Table 2) on photochemical properties depend on the solvents' polarities and coordinating power. In Table 2, there appears to be no distinct trend regarding solvent effects, however, Φ_Δ values for **5a** increased with an increase in the solvent polarity. With the exception of **5a**, Φ_Δ values are generally the lowest in $CHCl_3$, a feature attributed to the protic nature of the solvent. Solvent–singlet oxygen interactions in protic solvents have been found to cause deactivation of the singlet oxygen species formed, hence accounting for the low singlet quantum yields in such solvents [35].

S_Δ gives a measure of the efficiency of excitation energy transfer from the triplet state photosensitiser to ground state molecular oxygen. A value close to unity suggests high transfer efficiency. Values could only be determined in DMF, DMSO and toluene, due to the lack of suitable reference standards in $CHCl_3$ and THF. The data reflects relatively higher transfer efficiencies for **5a** and **5b** in toluene and DMSO compared to **6a** and **6b** in the same solvents, possibly a consequence of the position of the substituents on the Pc-ring (α-substitution versus β-substitution). Substitution at the peripheral positions possibly results in quenching of the triplet state also reflected in the lower triplet quantum yields discussed below (relative to those at the non-peripheral (α) positions). Table 2 shows that toluene exhibits in general, the lowest energy transfer efficiencies. This may be related to its low viscosity (Table 1) known to lead to enhanced excited state deactivation via external conversion [20], a process which may thus impede any energy transfer reactions from the excited states.

3.3.2. Photodegradation quantum yields

Photodegradation or photobleaching (Φ_{Pd}) is used to determine the photostability of MPc molecules and is identified by a decrease in the intensity of the absorption spectra without the appearance of new peaks. Photodegradation is a function of the nature of the substituents attached to the phthalocyanine periphery, the solvent and the central metal. The latter determines the lifetime of the molecule in the triplet state, which then determines the amount/rate of singlet oxygen production (responsible for the degradation of the Pc macrocycle). The photodegradation process generally involves oxidative attack of the MPc excited triplet state macrocycle by singlet oxygen via a Diels–Alder cycloaddition mechanism, the product of which is the respective substituted phthalimide [36,37]. Data shown in Table 2 indicates that photodegradation is more pronounced in $CHCl_3$ (except for complex **5b**). $CHCl_3$ tends to give the highest Φ_{Pd} values (more clear for peripherally substituted complexes **6**) due to its extremely low basicity (Table 1) which leaves the MPc molecule open to oxidative attack in this solvent [38–40]. DMSO, being a strongly coordinating and highly solvating solvent, is capable of axial coordination to the central metal atom thus partially shielding the Pc from oxidative attack [41]. Thus, the Φ_{Pd} values in DMSO are in general lower in comparison to those in non-coordinating and poorly coordinating solvents such as toluene, $CHCl_3$ and THF thus implying higher photostability of these complexes in strongly coordinating solvents than in non-coordinating and poorly coordinating solvents. DMSO is also more basic hence stabilizes the Pc ring against oxidative attack. Substituents may also confer some stability to the pc ring. However, electron-donating substituents enhance the probability of Pc ring photooxidation, while electron-withdrawing groups reduce it [42]. Substituents at non-peripheral (α) positions of the macrocycle are known to result in a stabilising effect an order of magnitude greater than substitution at the periphery (β) positions [42]. However, in Table 2, the non-peripherally substituted derivatives **5** showed less stability than the corresponding peripherally substituted derivatives **6** in toluene and THF, but the latter complexes are less stable in chloroform and conform to no particular trend in DMSO and DMF.

3.4. Photophysical studies

3.4.1. Fluorescence quantum yields

Fluorescence is strongly influenced by factors such as solvent polarity, viscosity, refractive index, temperature and molecular structural features. Fluorescence quantum yields (Φ_F) were calculated in all solvents as shown in Table 2. Higher Φ_F values were observed for α-derivatives compared to β-derivatives in THF, DMF, and $CHCl_3$. The trend was reversed in DMSO where large Φ_F values were obtained for the β-derivatives. Kobayashi et al. [8] have shown a shift of the Q-band to the red region is often accompanied by a lowering in Φ_F values, as is the case for complexes **5a** and **5b** in DMSO and toluene. In the case of $CHCl_3$, the large Φ_F values are unexpected as the presence of three Cl-atoms is expected to result in the lowest Φ_F values as a result of an induced spin-orbit coupling effect (induced by the heavy atom effect of the chlorines). Φ_F for **5a** and **5b** in DMSO are lower than in DMF, which could be explained by the presence of heavy sulphur atoms, which tend to enhance intersystem crossing to the triplet state, via spin-orbit coupling, and deactivate molecules against non-radiative transitions to the ground state. Φ_F values were consistently low in toluene. An increase in Φ_F values has been reported with the use of electron-donating nature of the substituents [42]. Table 2 generally shows lower Φ_F values for phenoxy (**b**)-substituted complexes compared to *t*-butylphenoxy (**a**).

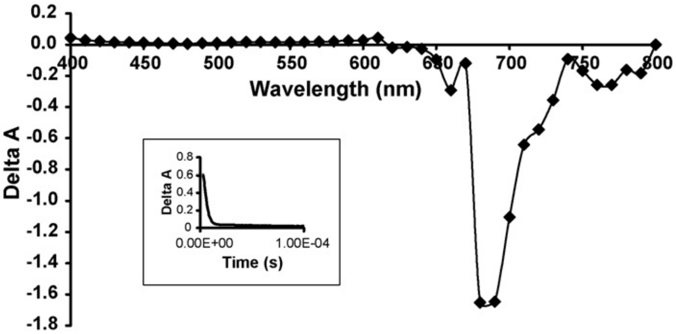

Fig. 5. Transient absorption spectrum for **6a** in toluene. Inset: **6b** triplet decay curve. Concentration: ~2.25×10^{-5} mol dm^{-3}; excitation wavelength (λ_{exc}) = 681 nm.

3.4.2. Triplet quantum yields and lifetimes

Population of the triplet state occurs in response to rapid intersystem crossing (ISC) from the excited singlet state. The triplet quantum yield (Φ_T) is thus used to quantify the fraction of molecules in the excited singlet state that undergo ISC to the triplet state. The insert shown in Fig. 5 shows a typical triplet decay curve using complex **6b** in toluene as an example. Since fluorescence and triplet yields are complimentary processes, low Φ_F values should be accompanied by a subsequent increase in values determined for Φ_T, and this is reflected by the data shown in Table 2 in toluene and DMSO. The trend is not clear in DMF. In DMF and DMSO, higher Φ_T were found for the α-substituted derivatives (**5a** and **5b**) than for the corresponding β-substituted derivatives (**6a** and **6b**). However, in toluene, the Φ_T values are lower for α-substituted derivatives compared to β-substituted ones. In toluene and DMSO, phenoxy-substituted derivatives give larger Φ_T values than *t*-butyl-substituted complexes; this is not the case in DMF. The highest Φ_T values were observed in toluene with values of 0.87 for **6b** and 0.76 for **6a**.

Shown in Fig. 5 is the transient absorption spectrum for **6a**. An important feature is the occurrence of peak broadening that occurs above 700 nm. Similar observations have been made with previous work on cadmium pyridyloxy complexes [11]. Such phenomena have been attributed to a change or slight loss in symmetry as a result of the attachment of flexible σ-bonded substituents (C–O–C bond between phenoxy substituents and

Pc-ring) as observed above for absorption. Partial degradation of the compounds, depicted by a decrease in absorption intensity, became evident on recording the absorption spectra following laser irradiations. Relatively long lifetimes (τ_T) were observed in DMSO ranging from 150 to 260 μs. These values are much higher than reported in DMSO for Cd tetra{2,(3)-pyridyloxyphthalocyanine complex where a value of 30 μs was obtained [11]. The τ_T values are expected to be low when the triplet quantum yields are larger. However, this is not the case in this work since the complexes gave the largest triplet yields in toluene, yet the τ_T values are low in this solvent compared to DMSO. Very low values (∼5 μs) were observed in the remaining solvents. The high viscosity of DMSO may [11] be used to account for this. High viscosity solvents cause more efficient deactivation of non-radiative transitions of excited state molecules, which normally occur in response to numerous diffusion-like molecular movements. Such movements are impeded in such highly viscous solvents, giving rise to the longer lifetimes experienced. *tert*-Butylphenoxy-substituted phthalocyanines employed in this work, i.e. **5a** (150 μs) and **6a** (260 μs) gave longer lifetimes when compared to the corresponding phenoxy-substituted derivatives; **5b** (130 μs) and **6b** (190 μs) in DMSO. Quantum yields of internal conversion (Φ_{IC}), have also been calculated but offer no additional information due to the lack of a well-defined pattern.

4. Conclusion

The work presented here has explored the effects of a variation in solvent, substituent type and position on the photophysicochemical properties of cadmium phthalocyanine complexes. The newly developed molecules demonstrate excellent solubility in high and low polarity organic solvents, i.e. DMSO, DMF, $CHCl_3$, THF and toluene. All the compounds studied exhibit intense red-absorption, typically between 670 and 700 nm and this coupled with the photochemical and photophysical data presented such good photostability, high Φ_T and relatively long τ_T, suggests that these complexes may prove to be useful as photocatalysts.

Acknowledgements

This work has been supported by the National Research Foundation of South Africa, Medical Research Council (MRC) and Rhodes University. WC thanks the Andrew Mellon Foundation and NRF for scholarships. EA thanks MRC for a post-doctoral bursary.

References

[1] M.J. Stillman, T. Nyokong, in: C.C. Leznoff, A.B.P. Lever (Eds.), Phthalocyanines: Properties and Applications, vol. 1, VCH Publications, New York, 1993 (Chapter 3).
[2] J. Mack, M.J. Stillman, J. Porphyrins Phthalocyanines 5 (2001) 67.
[3] T.C. Vancott, J.L. Rose, G.C. Misener, B.E. Williamson, A.E. Schrimpf, M.E. Boyle, P.N. Schatz, J. Phys. Chem. 93 (1989) 2999.
[4] P. Turek, P. Petit, J.-J. Andre, J. Simon, R. Even, B. Boudjema, G. Guillaud, M.-J. Maitrot, J. Am. Chem. Soc. 109 (1987) 5119.
[5] R. Li, X. Zhang, P. Zhu, D.K.P. Ng, N. Kobayashi, J. Jiang, Inorg. Chem. 45 (2006) 2327.
[6] N.B. McKeown, in: K.M. Kadish, K.M. Smith, R. Guilard (Eds.), The Porphyrin Handbook, vol. 15, Academic Press, New York, 2003 (Chapter 98).
[7] H. Schultz, M. Lehman, M. Rein, M. Hanack, Struct. Bond. 74 (1991) 41.
[8] N. Kobayashi, H. Ogata, N. Nonaka, E.A. Luk'yanets, Chem. Eur. J. 9 (2003) 5123.
[9] N. Kobayashi, N. Sasaki, Y. Higashi, T. Osa, Inorg. Chem. 34 (1995) 1636.
[10] K. Ban, K. Nishizawa, K. Ohta, H. Shirai, J. Mater. Chem. 10 (2000) 1083.
[11] W. Chidawanyika, A. Ogunsipe, T. Nyokong, New J. Chem. 31 (2007) 377.
[12] Z.A. Bayir, E. Hamuryudan, A.G. Gurek, Ö. Bekaroğlu, J. Porphyrins Phthalocyanines 1 (1997) 349.
[13] W.-F. Law, R.C.W. Liu, J. Jiang, D.K.P. Ng, Inorg. Chim. Acta 256 (1997) 147.
[14] S. Foley, G. Jones, R. Liuzzi, D.J. McGarvey, M.H. Perry, T.G. Truscott, J. Chem. Soc. Perkin Trans. 2 (1997) 1725.
[15] P. Tau, T. Nyokong, Polyhedron 25 (2006) 1802.
[16] M. Durmus, T. Nyokong, Tetrahedron 63 (2007) 1385.
[17] J. Kossanyi, D. Chahraoui, Int. J. Photoenergy 2 (2000) 9.
[18] W. Spiller, H. Kliesch, D. Wõrhle, S. Hackbarth, B. Roder, G. Schnurpfeil, J. Porphyrins Phthalocyanines 2 (1998) 145.
[19] L. Kaestner, M. Cesson, K. Kassab, T. Christensen, P.D. Edminson, M.J. Cook, I. Chambrier, G. Jori, Photochem. Photobiol. Sci. 2 (2003) 660.
[20] A. Ogunsipe, D. Maree, T. Nyokong, J. Mol. Struct. 650 (2003) 131.
[21] H. Tomada, S. Saito, S. Shiraishi, Chem. Lett. 12 (1983) 313.
[22] S. Fery-Forgues, D. Lavabre, J. Chem. Educ. 76 (1999) 1260.
[23] J. Fu, X.Y. Li, D.K.P. Ng, C. Wu, Langmuir 18 (2002) 3843.
[24] P. Kubát, J. Mosinger, J. Photochem. Photobiol. A: Chem. 96 (1996) 93.
[25] T.H. Tran-Thi, C. Desforge, C. Thiec, J. Phys. Chem. 93 (1989) 1226.
[26] P. Kubat, J. Mosinger, J. Photochem. Photobiol. A 96 (1996) 93.
[27] S.M. Bishop, A. Beeby, A.W. Parker, M.S.C. Foley, D. Phillips, J. Photochem. Photobiol. A 90 (1995) 39.
[28] T.M. Keller, T.R. Price, J.R. Griffith, Synthesis 74 (1980) 613.
[29] W.M. Sharman, J.E. van Lier, in: K.M. Kadish, K.M. Smith, R. Guilard (Eds.), The Porphyrin Handbook, vol. 15, Academic Press, New York, 2003 (Chapter 97).
[30] N. Kobayashi, J. Mack, K. Ishii, M.J. Stillman, Inorg. Chem. 41 (2002) 5350.
[31] A.L. Maclean, G.J. Foran, B.J. Kennedy, P. Turner, T.W. Hambley, Aust. J. Chem. 49 (2002) 352.
[32] K. Kasuga, N. Matsuura, K. Inone, M. Handa, T. Sugimori, K. Isa, M. Nakata, Chem. Lett. (2002) 352.
[33] N. Kobayashi, T. Fukuda, K. Ueno, H. Ogino, J. Am. Chem. Soc. 123 (2001) 10740.
[34] A. Ogunsipe, T. Nyokong, J. Mol. Struct. 689 (2004) 89.
[35] R. Bonnett, Chemical Aspects of Photodynamic Therapy, Gordon and Breach Science, Canada, 2000.
[36] A.K. Sobbi, D. Wõhrle, D. Schlettwein, J. Chem. Soc. Perkin. Trans. 2 (1993) 481.
[37] M.J. Cook, I. Chambrier, S.J. Cracknell, D.A. Mayes, D.A. Russell, Photochem. Photobiol. 62 (1995) 542.
[38] A. Ogunsipe, J.-Y. Chen, T. Nyokong, New J. Chem. 28 (2004) 822.
[39] J. Grodkowski, J.H. Chambers Jr., P. Neta, J. Phys. Chem. 88 (1984) 5332.
[40] N.A. Kuznetsova, V.V. Okunchikov, V.M. Derkacheva, O.L. Kaliy, E.A. Luk'yanets, J. Porphyrins Phthalocyanines 9 (2005) 393.
[41] G. Winter, H. Heckmann, P. Haisch, W. Eberhardt, M. Hanack, L. Lüer, H.-J. Egelhaaf, D. Oelkrug, J. Am. Chem. Soc. 120 (1998) 11663.
[42] H. Xu, T. Shen, O. Zhou, S. Shen, J. Liu, L. Li, S. Zhou, X. Zhang, Q. Yu, Z. Bi, X. Xias, J. Photochem. Photobiol. A: Chem. 65 (1992) 267.
[43] J. Catalán, C. Díaz, V. López, P. Pérez, J.-L.G. de Paz, J.G. Rodríguez, Liebigs Ann. (1996) 1785.
[44] O.W. Kolling, Anal. Chem. 54 (1982) 260.
[45] V. Gutmann, Electrochim. Acta 21 (1976) 661.